

9C seismic modelling for VTI media

Ritesh K. Sharma* and Robert J. Ferguson, University of Calgary

SUMMARY

An extrapolation method is presented for modelling 3D-9C seismic data in media that are transversely anisotropic. Fourier decomposition is used so that wavefield extrapolation proceeds as a set of distributed, monochromatic extrapolation steps in depth. Three component (3C) geophones are implemented on each grid point of the horizontal reflecting surface. A 3C model source wavefield is extrapolated by 3D phase shift operators in anisotropic media to each grid point. There, a rotation matrix transforms the source polarization into the orientation of the multicomponent geophone. The polarization angle (dip) of the incident compressional wave and the horizontal projection of the associated slowness vector at each grid point are the essential parameters of a rotation matrix. Travel times in anisotropic media are accommodated through plane wave transformation and phase shift, and a propagation angle is produced. For each geophone component, the polarization angle is calculated from the propagation angle. Synthetic examples are given to demonstrate this approach.

INTRODUCTION

Wave field extrapolation in the plain wave domain insures efficiency in terms of computational time (Sharma and Ferguson, 2009). Given a source type, the source wavefield is extrapolated from the earth surface to reflector as

$$\varphi_{\Delta z} = \varphi_0 e^{i\Delta z q \omega} \quad (1)$$

where φ_0 is the spectra of the source wavefield at the surface obtained via the Fast Fourier Transform (FFT) ($t \rightarrow \omega$, $x \rightarrow p_1 \omega$, $y \rightarrow p_2 \omega$) of the source wavefield. Source wavefield $\varphi_{\Delta z}$ is the wavefield at depth Δz after extrapolation. q is the vertical slowness and depends on the seismic velocity and horizontal slownesses p_1 and p_2 through the scalar wave-equation. In transverse isotropic (TI) media, q depends on a set of elastic coefficients - α_0 , β_0 , δ , ϵ , and γ . q is also known for different seismic wave modes in anisotropic media (Ferguson and Margrave, 2008).

After extrapolation, the source wavefield resides on the reflecting plane. Together, the polarization directions of P-, SV-, and SH-waves (compression, vertical shear, and horizontal shear respectively) characterize a 3 dimensional co-ordinate system defined here as the survey co-ordinate system while the recording coordinate system is characterized by the three component directions of a 3C geophone.

THEORY

To model the arrival of a 3C wave, we rotate the survey coordinate system to register the source energy on the vertical, in-line, and cross-line components. With the basic method

of a co-ordinate systems transformation (Neufeld and Clayton, 2000), we transform the survey coordinate system into the recording system by rotation θ degrees about the x axis followed by a rotation ϕ degrees about the z axis. These angles are defined pictorially in Figure 1. A hypothetical geophone indicated by three orthogonal blue lines is aligned with spacial axes x , y , and z . The normal to an incident plane wave is indicated by symbol I , and the horizontal projection of I is indicated by H_p . Azimuth ϕ is indicated on this figure, and dip angle θ is the angle between I and z .

Angle θ is the angle that the polarization vector of an incident planewave makes with the vertical component of a 3C geophone. The slowness vector $\hat{\mathbf{p}}$ characterizes the direction of the incident wavefield according to (Ferguson and Margrave, 2008),

$$\hat{\mathbf{p}} = \frac{p_1 \hat{\mathbf{i}} + p_2 \hat{\mathbf{j}} + q \hat{\mathbf{k}}}{\sqrt{p_1^2 + p_2^2 + q^2}}, \quad (2)$$

where p_1 , p_2 and q are the horizontal components and vertical component of $\hat{\mathbf{p}}$ respectively. The unit normal associated with a 3C geophone at a grid location is

$$\hat{\mathbf{a}} = \sin \theta_a \cos \phi_a \hat{\mathbf{i}} + \sin \theta_a \sin \phi_a \hat{\mathbf{j}} + \cos \theta_a \hat{\mathbf{k}}, \quad (3)$$

where θ_a and ϕ_a are the dip and azimuth of the normal to the interface respectively.

The angle θ between $\hat{\mathbf{p}}$ and $\hat{\mathbf{a}}$ is then computed by cross product according to (Ferguson and Margrave, 2008)

$$\sin \theta = |\hat{\mathbf{p}} \times \hat{\mathbf{a}}|, \quad (4)$$

where \times indicates cross product. Note, though we restrict our discussion here to horizontal interfaces ($\hat{\mathbf{a}} = \hat{\mathbf{k}}$) for simplicity, we anticipate implementation of dipping interfaces as an extension to this approach.

Propagation angle θ , once computed, is used to calculate the polarization angle in terms of elastic coefficients (Slawinski, 2003, for example). We develop a relationship between these two angles in terms of Thomson parameters Thomsen (1986) according to

$$\theta_1 = \tan^{-1} \frac{(\alpha^2(\theta) - \beta_0^2 \sin^2 \theta - \alpha_0^2 \cos^2 \theta)}{\sqrt{[\alpha_0^2 - \beta_0^2] [\alpha_0^2 [2\delta + 1] - \beta_0^2]} \sin \theta \cos \theta} \quad (5)$$

for P-waves for example, where θ_1 is the polarization angle, θ is the propagation angle computed from equation 4, and $\alpha(\theta)$ is the anisotropic P-wave velocity. Given θ_1 and a known source, effective 3C recording V_{θ_1} is computed

$$V_{\theta_1} = \begin{bmatrix} 1 & 0 & 0 \\ 0 & \cos \theta_1 & \sin \theta_1 \\ 0 & -\sin \theta_1 & \cos \theta_1 \end{bmatrix} W, \quad (6)$$

where W describes the known source type. Generally, a 3C

Forward Modelling

source wavefield is written in matrix form as (Ferguson, 2009)

$$W = \begin{bmatrix} s_1 \\ s_2 \\ w \end{bmatrix} \quad (7)$$

where s_1 , s_2 and w are the cross-line, in-line and vertical components of the source respectively. A vertical source wavefield, for example, is written

$$W = \begin{bmatrix} 0 \\ 0 \\ w \end{bmatrix}. \quad (8)$$

Figure 2 depicts four 3C geophones positioned at grid points 200 m below a source position. Rotation θ_1 degrees about the x axis (H_1) is anti-clockwise for geophones to the left of the source and clockwise for geophones to the right. So, we adopt the convention of a positive angle for anti-clockwise rotation and negative for clockwise rotation (Neufeld and Clayton, 2000).

Azimuth ϕ is the angle between one of the horizontal geophone components and the plane made with the source, and it is calculated from the input parameters of a plane wave. Following rotation θ_1 degrees about the x axis, the source waveform is rotated ϕ degrees about the vertical axis. A rotation ϕ about the vertical axis is computed and is written as

$$V_\phi = \begin{bmatrix} \cos \phi & \sin \phi & 0 \\ -\sin \phi & \cos \phi & 0 \\ 0 & 0 & 1 \end{bmatrix} W. \quad (9)$$

As a single operation, rotation through θ_1 and ϕ is computed as

$$V = \begin{bmatrix} \cos \phi & \sin \phi \cos \theta_1 & \sin \theta_1 \sin \phi \\ -\sin \phi & \cos \phi \cos \theta_1 & \cos \phi \sin \theta_1 \\ 0 & -\sin \theta_1 & \cos \theta_1 \end{bmatrix} W, \quad (10)$$

where V is the source wavefield rotated into the orientation of the 3C geophone. Normally it is written as (Ferguson, 2009)

$$V = \begin{bmatrix} H_1 \\ H_2 \\ Z \end{bmatrix} \quad (11)$$

where H_1 , H_2 , and Z are the cross-line, in-line and vertical components of the vector wavefield respectively.

EXAMPLES

As a simple demonstration, a numerical model of a 700m thick VTI medium (shale) is constructed. The anisotropic parameters of this shale in Thomson (Thomsen, 1986) parameters are $\alpha_0 = 3048$ m/s, $\beta_0 = 1490$ m/s, $\epsilon = 0.255$, $\delta = -0.27$, and $\gamma = 0.480$.

Figures 3(a), 3(b), and 3(c) show the in-line slice of 3D data from a P-wave source obtained through the procedure outlined above. The circle in the top right of Figure 3(c) is the plan view of a recording surface where the source location is in the centre at the origin. (Data in this Figure, and all subsequent

Figures, correspond to this geometry.) In-line and cross-line directions are indicated by horizontal and vertical axis of this circle, and the dashed red line indicates the direction along which a vertical slice through the modelled data is taken.

On the middle traces, energy registers strongest on the Z (3(c)) and H_1 (3(a)) components as expected (the slice is offset in the H_1 direction from the source). Note, the (a), (b), and (c) correspondence with H_1 , H_2 , and V , is consistent hereafter in all Figures. Traces out from the middle have more energy on H_2 (3(b)), and energy decreases on Z and H_1 . Polarity on the H_2 component flips from on either side of the source, while polarity is stationary on Z and H_1 .

An in-line slice for an SH source is shown in Figures 4(a), 4(b), and 4(c). No energy registers on the Z or the H_1 components closest to the source, and there is strong registration of energy on H_2 . Away from the source, energy registers strongest on the H_1 component as expected.

Figures 5(a), 5(b), and 5(c) demonstrates an interesting property possessed by SV-waves generated by an SV-source. For anisotropic media, SV-waves triplicate (exhibit three arrivals) when the thickness of the anisotropic medium is significant (Ferguson and Sen, 2004, for example), and this is strongly apparent on Z and H_2 . Close to the source, energy registers on H_1 and H_2 , and away from the source, more energy is registered Z . Polarity on H_2 reverses on either side of the source.

CONCLUSIONS

Forward modelling of 9C seismic data for VTI media is done after applying a rotation matrix on the extrapolated wavefield. At zero offset (a point where dashed red line crosses the vertical axis of circle) energy is registered only on H_1 and the vertical component when a pure compression wave source is used. The registration of energy increases with offset on the H_2 component. In using a cross-line source, H_2 component is more favorable for recording energy at zero offset and energy registration increases on the H_1 component with increasing offset. The phenomenon of triplication occurs in using an in-line source. This is supported by another approach also. The vertical component is more favorable for energy registration at far offset in this case.

ACKNOWLEDGMENT

I wish to thank sponsors, faculty and staff of CREWES, and the Natural Sciences and Engineering Research Council of Canada (NSERC, CRDPJ 379744-08), for their support of this work.

Forward Modelling

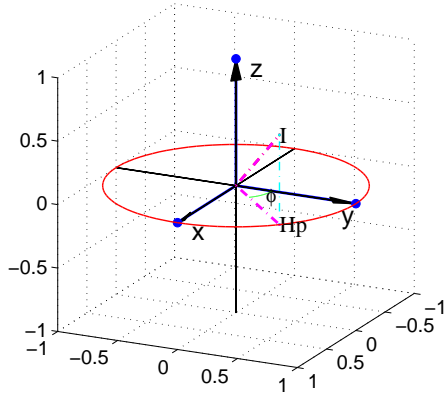


Figure 1: Schematic representation of source wavefield incident on 3C geophone at a single grid point.

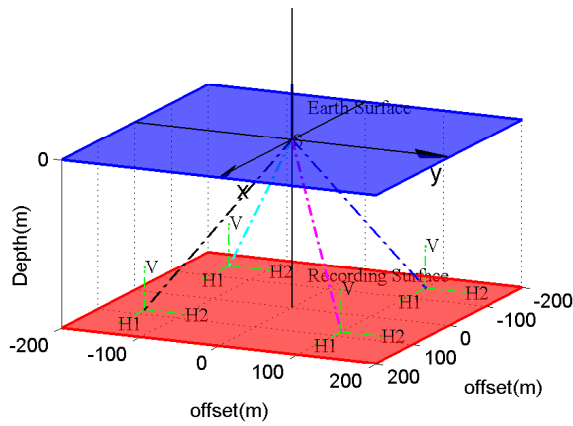


Figure 2: Schematic representation of considered model and positioning of 3C geophones at reflecting surface.

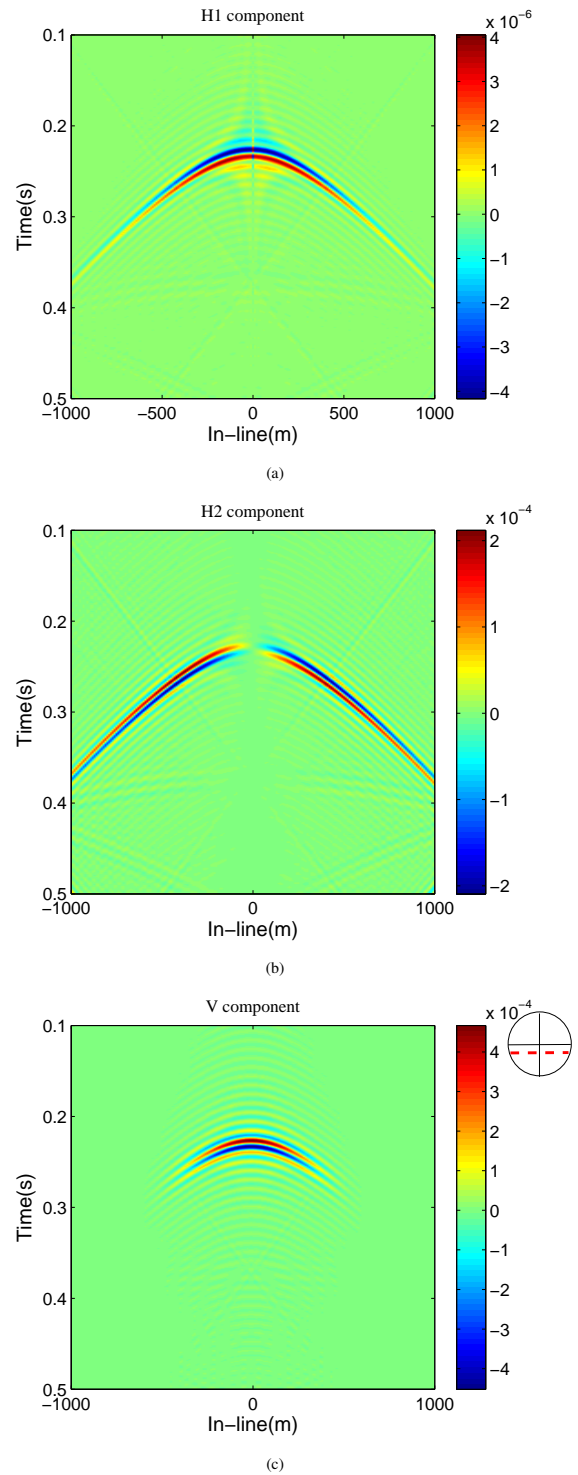


Figure 3: (a) H1 component (b) H2 component and (c) Vertical component of an in-line slice of 3D data when a *P*-wave source is used at the surface. The plan view of recording surface is indicated by the circle on the top. The dashed red line is the direction along which slice is taken.

Forward Modelling

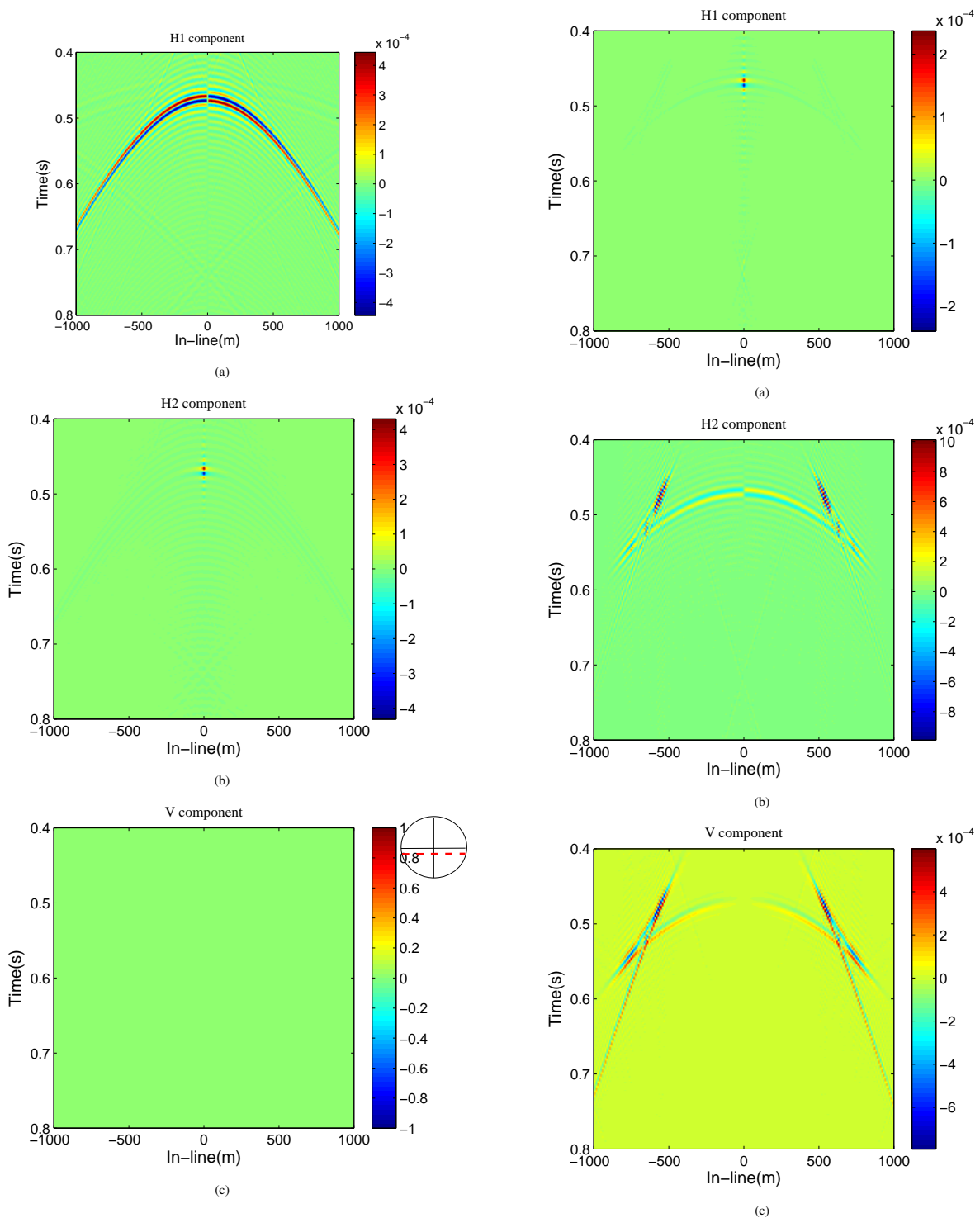


Figure 4: In-line slice of 3D seismic data represented by components (a) H1 (b) H2 and (c) Vertical. SH source is used at the surface.

Figure 5: Schematic representation of components (a) H1 (b) H2 and (c) Vertical of an in-line slice of 3D seismic data obtained using SV source at the surface.